Particle-in-cell simulations of magnetically driven reconnection using laser-powered capacitor coils

Kai Huang, Quanming Lu, Lan Gao, Hantao Ji, Xueyi Wang, and Feibin Fan

Citation: Physics of Plasmas **25**, 052104 (2018); doi: 10.1063/1.5021147
View online: https://doi.org/10.1063/1.5021147
View Table of Contents: http://aip.scitation.org/toc/php/25/5
Published by the American Institute of Physics

Particle-in-cell simulations of magnetically driven reconnection using laser-powered capacitor coils

Kai Huang,[1] Quanming Lu,[1,a)] Lan Gao,[2] Hantao Ji,[2,3] Xueyi Wang,[4] and Feibin Fan[1]
[1]*CAS Key Laboratory of Geospace Environment, Department of Geophysics and Planetary Science, University of Science and Technology of China, Hefei 230026, China*
[2]*Princeton Plasma Physics Laboratory, Princeton University, Princeton, New Jersey 08543, USA*
[3]*Department of Astrophysical Sciences, Princeton University, Princeton, New Jersey 08544, USA*
[4]*Physics Department, Auburn University, Auburn, Alabama 36849, USA*

(Received 2 January 2018; accepted 14 April 2018; published online 7 May 2018)

In this paper, we propose an experimental scheme to fulfill magnetically driven reconnections. Here, two laser beams are focused on a capacitor-coil target and then strong currents are wired in two parallel circular coils. Magnetic reconnection occurs between the two magnetic bubbles created by the currents in the two parallel circular coils. A two-dimensional particle-in-cell simulation model in the cylindrical coordinate is used to investigate such a process, and the simulations are performed in the (r, z) plane. The results show that with the increase of the currents in the two coils, the associated magnetic bubbles expand and a current sheet is formed between the two bubbles. Magnetic reconnection occurs when the current sheet is sufficiently thin. A quadrupole structure of the magnetic field in the θ direction (B_θ) is generated in the diffusion region and a strong electron current along the r direction (J_{er}) is also formed due to the existence of the high-speed electron flow away from the X line in the center of the outflow region. Because the X line is a circle along the θ direction, the convergence of the plasma flow around $r = 0$ will lead to the asymmetry of J_{er} and B_θ between the two outflow regions of magnetic reconnection. *Published by AIP Publishing.* https://doi.org/10.1063/1.5021147

I. INTRODUCTION

Magnetic reconnection not only provides a physical mechanism for fast conversion from magnetic energy to plasma kinetic energy, but also can accelerate and heat charged particles and produce energetic particles.[1–6] It is generally accepted that magnetic reconnection is the key to unveil the mystery of explosive phenomena in space plasma, like solar flares and substorms in the earth's magnetosphere.[7–10] Therefore, magnetic reconnection has always been a hot topic in space plasma since the first physical model was proposed in 1950s independently by Sweet and Parker.[1,11]

Besides satellite observations, well-designed laboratory experiments provide another experimental platform to study magnetic reconnection.[12] For example, MRX (Magnetic Reconnection Experiment) has made much progress on the structures of the ion diffusion region and associated plasma waves with magnetic reconnection.[13,14] Recently, a magnetic reconnection experiment has been realized in high-energy-density laser-driven plasmas.[15–18] In such an experiment, magnetic reconnection occurs between two expanding plasma bubbles with the azimuthal magnetic field. The plasma bubbles are created by two closely focused laser beams on a plane foil target, and the azimuthal magnetic field is self-generated through a noncollinear electron density and temperature gradient. The expanding speed of the plasma bubbles is usually several times of the sound speed and the plasma beta is $\sim$10.[19–22] Therefore, the expanding speed is much larger than the Alfven speed, and the process of interaction between the plasma bubbles can be roughly separated into two stages: in the first stage, the two plasma bubbles expand quickly and collide with each other, which leads to the enhancement of the magnetic field in the inflow region and the acceleration of energetic electrons mainly due to Fermi and betatron mechanisms; in the second stage, the magnetic field lines from the plasma bubbles begin to reconnect and energetic electrons are mainly produced due to the reconnection electric field in the vicinity of the X line.[23] Magnetic islands may be generated due to the tearing mode in the second stage when the formed current sheet is sufficiently thin,[18,20] and electrons will suffer further acceleration when trapped in these islands,[23,24] which has also been discussed before during reconnection in a Harris current sheet.[25,26] When the expanding speed is sufficiently large, the spectrum of energetic electrons at higher energy has a power law distribution.[27]

Recently, kinetic simulations of magnetic reconnection have revealed that energetic electrons tend to be accelerated with more efficiency with the decrease of the plasma beta and produce a power law distribution.[28,29] Fulfilling experimental magnetic reconnection in a laser-driven plasma with a low beta is now attracting more and more attention. One way is to drive two plasma plumes prefilled with a low-density background plasma and the external magnetic field by two plasma bubbles created by two closely focused laser beams on a plane foil target, and magnetic reconnection occurs when the external magnetic field embedded in the two plumes has an opposite direction.[30] Another way is to wire two parallel coils with parallel currents by focusing

a)Author to whom correspondence should be addressed: qmlu@ustc.edu.cn

laser beams on a capacitor-coil target that comprises two parallel metallic foils, and magnetic reconnection occurs between two magnetic bubbles created by the currents in the two parallel coils.[31] Generating a magnetic field using a laser-powered capacitor-coil target was firstly carried out by Daido *et al.* in 1986,[32] where the measured magnetic field can be up to 60 T at the center of a one-turn coil. The amplitude of the generated magnetic field with such a technique was measured to be from tens of tesla to kilotesla.[33–35] Thanks to the progress, it becomes feasible to study reconnection in a low beta plasma using a laser-powered capacitor-coil. Pei *et al.*[31] demonstrated a plasma device for experimental magnetic reconnection between two plasma plumes with the magnetic fields created by two parallel U-turn coils, which are driven by irradiating Gekko XII lasers for a double-turn Helmholtz capacitor target, and they observed an accumulation of plasma plume in the outflow region.

Here, in this paper, we propose a new experimental scheme to fulfill magnetic reconnection, which is magnetically driven by two parallel circular coils powered by irradiating lasers to a capacitor target. Different from Pei *et al.*,[31] here, we use two circular coils, instead of U-turn coils, to drive magnetic reconnection. In our scheme, the driven reconnection has an axisymmetric and primarily two-dimensional (2-D) geometry. It allows better plasma confinement via the periodic boundary condition in the toroidal direction and more efficient particle acceleration. We also investigate the corresponding characteristics of the proposed reconnection with a 2-D particle-in-cell (PIC) simulation model in the cylindrical coordinate. The experimental scheme and the simulation model are described in Sec. II. Section III presents the simulation results and we give the summary and discuss the simulation results in Sec. IV.

II. EXPERIMENTAL SCHEME AND SIMULATION MODEL

We propose a new experimental scheme, where magnetic reconnection occurs between two laser-powered parallel coils. The scheme is shown in Fig. 1. Two laser beams are focused on the capacitor-coil target, which has two connecting circular coils in parallel to each, and they will propagate through the laser entrance holes on the front plate and focused on the back-plate foil. One particular addition is that there is a rectangular spacer between the two plates to block the plasma expanding into the reconnection region. The electrical potential generated by hot electrons leaves the back plate and streams onto the front plate. The coils are then wired and drive strong currents in the two parallel circular coils. As a result, an axisymmetric magnetic reconnection geometry of anti-parallel magnetic fields will be created, with a circular toroidal current sheet between the two circular coils. Before the magnetic fields are induced in the coils, a low-density tenuous plasma will be filled in the coil region by irradiating a low-intensity laser onto a foam target.

A 2-D PIC simulation model in the cylindrical coordinate is used in this paper to investigate such kind of magnetic reconnection and the simulation is performed in the (r, z) plane, as shown in Fig. 2. The particles move in the (r, z) plane and their velocities have three components (v_r, v_z, v_θ). The electromagnetic fields also have three components and their derivative along the θ direction is zero $(\partial/\partial\theta = 0)$. The conducting boundary condition is used for electromagnetic fields in both the r and z directions, while particles are assumed to be reflected into the simulation domain when they leave the boundaries in both the r and z directions. The three-dimensional (3-D) effects, such as the kink mode in the θ direction, cannot be considered in our simulation model.

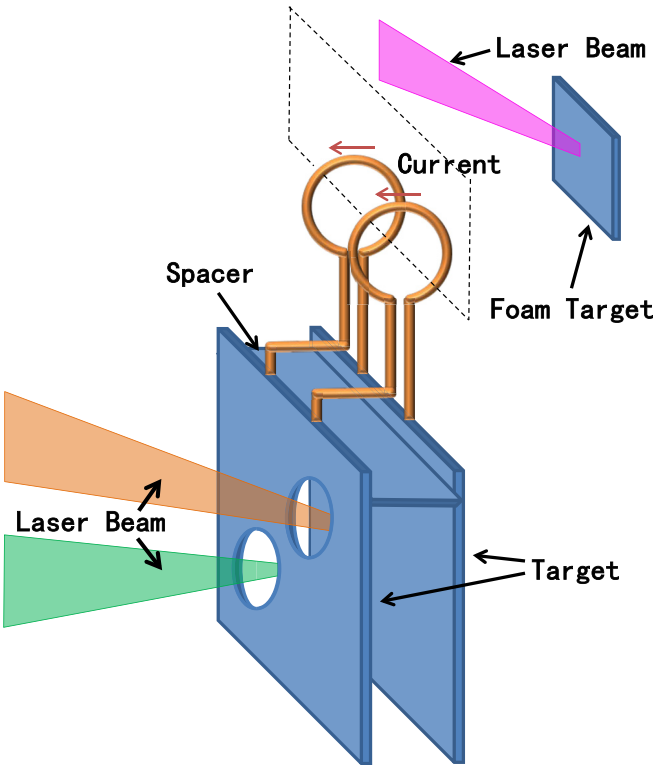

FIG. 1. Proposed experimental scheme for axisymmetric magnetic reconnection using the laser-driven capacitor-coil targets. The dashed line box is the simulation domain.

The experimental parameters are assumed to have the following values: the radius of the coils is $R = 300\,\mu$m and the distance between the two coils is $D = 500\,\mu$m. The shape of the wire is a square with the side length $l = 50\,\mu$m.

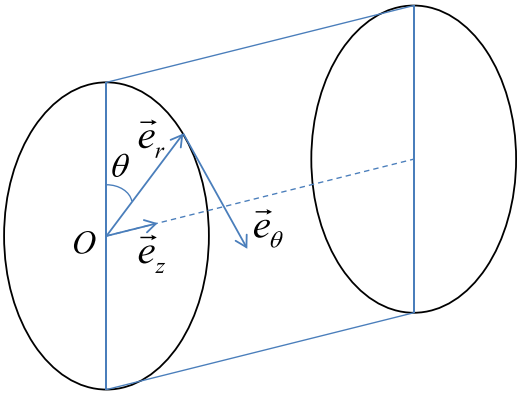

FIG. 2. The cylindrical coordinate used in the 2-D PIC simulation model, which is performed in the (r, z) plane.

Because the side length of the square is much smaller than both the distance between the two coils and the radius of the coils, the effects of the exact shape of the wire on the resulting magnetic reconnection are negligible. The background electron density is $n_{e0} = 1 \times 10^{18}\,\mathrm{cm}^{-3}$ and the ions and electrons have the same temperature, which is $T_{e0} = T_{i0} = 200\,\mathrm{eV}$. The target mixes 50% C and 50% H, the ion mass expressed in units of the proton mass is $A = m_i/m_p = 10$, and the average ionic charge is $Z = 5$. Therefore, the background ion density $n_{i0} = 2 \times 10^{17}\,\mathrm{cm}^{-3}$ and the ion inertial length is $d_i \approx 320\,\mu\mathrm{m}$. Recently, Fiksel *et al.*[36] proposed a model to estimate the evolution of the current in a laser-powered coil based on the laser parameters, and it can be roughly considered to have two stages: a linear increase in the peak, followed by exponential decay. In our simulations, we simply use such a kind of evolution of the current in the coils as a parameter, instead of the laser parameters. The peak current is assumed to be $I_0 = 30\,\mathrm{kA}$ in our simulations. Such a current can produce the magnetic field and the amplitude is $B_0 = 24\,\mathrm{T}$ at the distance $D/2$ from the center of the wire. The electron plasma beta is $\beta_{e0} = 2\mu_0 n_{e0} k_B T_{e0}/B_0^2 \approx 0.125$. The details of these physical parameters are listed in Table I. According to these parameters, the estimated electron mean free path is about 600 μm, which is larger than the measured width of the current layer. Therefore, the plasma can be considered as collisionless and modelled with PIC simulations.

In our simulation, the domain size is $[-L_z, L_z] \times [-L_r, L_r]$. $L_z = 3d_i$ and $L_r = 4d_i$ (where d_i is the ion inertial length based on n_{i0}). The grid number is $N_z \times N_r = 300 \times 400$ and the grid size is $\Delta z = \Delta r = 0.02d_i$. The ion-to-electron mass ratio Zm_i/m_e is 100 and the light speed is $c = 20V_A$ (where V_A is the Alfven speed based on B_0 and n_{i0}). We choose the radius of the coils as $R = 1.0d_i$ and the distance between the two coils $D = 1.67d_i$. The current is divided into external current and plasma current. The external current is defined on the grids corresponding to the coils and varies with time and the plasma current is calculated by counting particles. Cubic interpolation is used to deposit charge and current. If there is no explicit statement, the linear rising time of the current in the coils is $T_r = 2\Omega_{i0}^{-1}$ and the exponential decay time is $T_d = 6\Omega_{i0}^{-1}$. The initial ion and electron temperatures are $T_{e0} = T_{i0} = 0.016 m_e c^2$. The time step is $\Delta t = 0.0001\Omega_{i0}^{-1}$ (where $\Omega_{i0} = ZeB_0/m_i$ is the ion gyrofrequency). The initial plasma density is assumed to be uniform and 200 particles per species in a grid for n_{i0} are employed in the simulations.

TABLE I. Estimated physical parameters.

Parameter	Estimated values
Ions	CH (50% C and 50% H)
Average ionic charge Z	5
Background electron density n_{e0}	$1 \times 10^{18}\,\mathrm{cm}^{-3}$
Background ion density n_{i0}	$2 \times 10^{17}\,\mathrm{cm}^{-3}$
Temperature $T_e = T_i$	200 eV
Magnetic field B_0	24 T
Radius of the coils R	300 μm
Distance between the two coils D	500 μm
Ion inertial length d_i	320 μm
Ion gyrofrequency Ω_{i0}	1.15×10^9/s
Alfven speed V_A	371 km/s
Electron plasma beta β_{e0}	0.125

III. SIMULATION RESULTS

Figure 3 shows the magnetic field B and the electron current in the θ direction $J_{e\theta}$ at $\Omega_{i0}t =$ (a) 1.0, (b) 2.0, (c) 3.0, and (d) 6.0. With the increase in the current in the coils, the produced magnetic field forms two separated bubbles, which expand continuously. During the expansion of the two bubbles, the electron current in the θ direction is generated at the edge of the bubbles, where the electrons are accelerated by the resulting motional electric field. Such a process is similar to the acceleration of the reflected particles by a shock front.[37] Then, at about $\Omega_{i0}t = 2.0$, a thin current sheet is formed between the two bubbles. At last, the magnetic field lines from the two bubbles reconnect at about $\Omega_{i0}t = 2.7$. The whole process can also be clearly depicted in Fig. 4, which plots the time evolution of the (a) magnetic flux function Φ_B, (b) magnetic field B and (c) electron current in the θ direction $J_{e\theta}$ along $r = 1.0$, which crosses the X line when magnetic reconnection occurs between the magnetic field lines from the two bubbles. A thin current sheet with the half width of about 0.2 d_i begins to form between the two plasma bubbles at about $\Omega_{i0}t = 2.0$, and it lasts about $1.0\Omega_{i0}^{-1}$. Then, with the progression of magnetic reconnection, the current sheet becomes wider and wider and the diffusion region around the X line also expands.

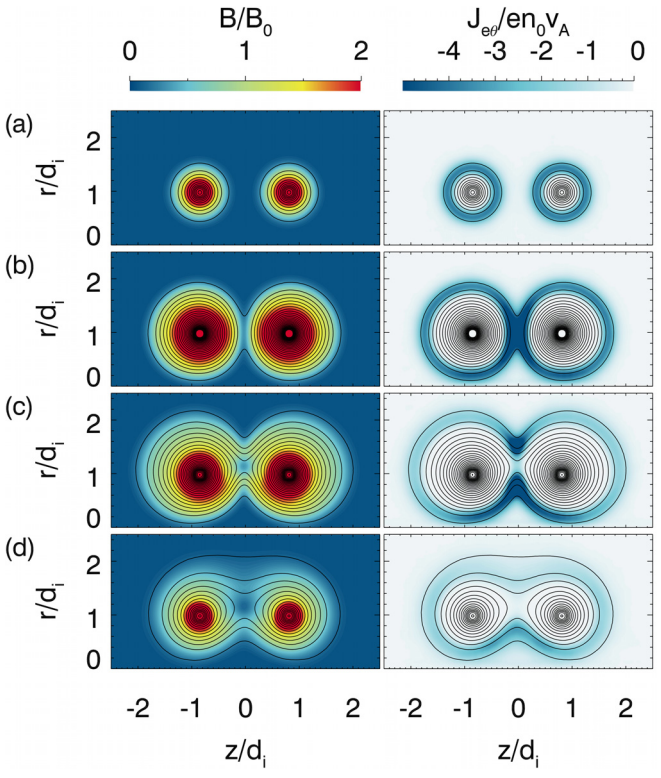

FIG. 3. The magnetic field B/B_0 and the electron current in the θ direction $J_{e\theta}/en_0v_A$ at $\Omega_{i0}t =$ (a) 1.0, (b) 2.0, (c) 3.0, and (d) 6.0.

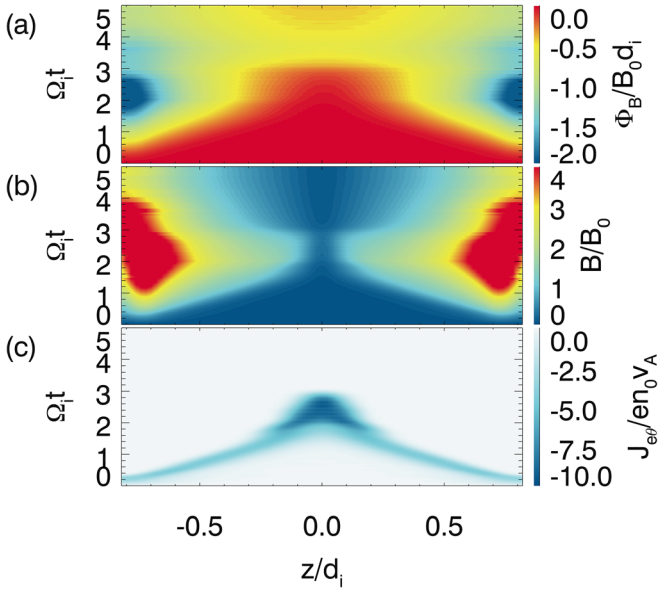

FIG. 4. The time evolution of the (a) magnetic flux function $\Phi_B/B_0 d_i$, (b) magnetic field B/B_0 and (c) out-of-plane electron current density $J_{e\theta}/en_0v_A$ along $r = 1.0$, which crosses the X line.

Figure 5 exhibits the distributions of (a) the magnetic field in the θ direction B_θ, (b) the electric field in the θ direction E_θ, and (c) the electron current in the r direction J_{er} at $\Omega_{i0}t = 3.0$. The reconnection electric field can be obviously identified in the vicinity of the X line. A quadruple structure of B_θ exists around the X line and the electron current J_{er} is directed toward the X line in the outflow region. The generation of J_{er} in the outflow region is attributed to the fast motion of the magnetic field lines away from the X line. The

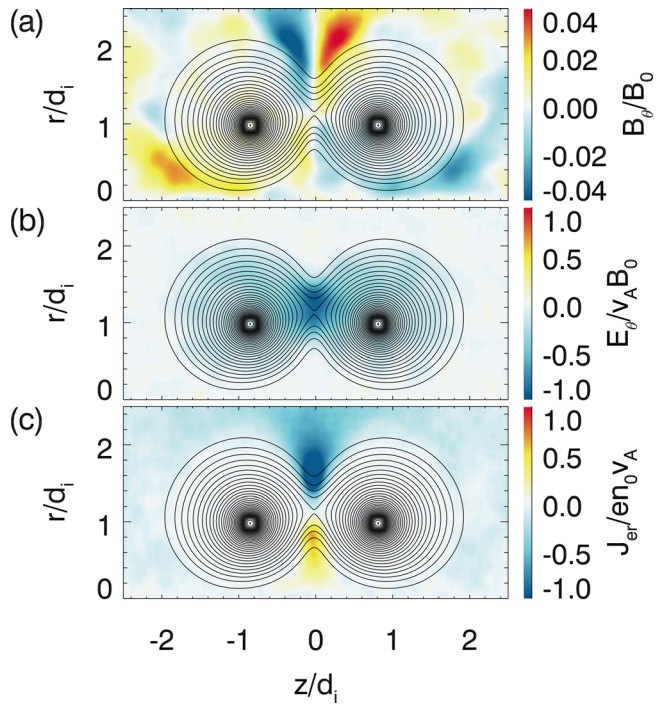

FIG. 5. The distributions of (a) the magnetic field in the θ direction B_θ/B_0, (b) the electric field in the θ direction E_θ/v_AB_0, and (c) the electron current in the r direction J_{er}/en_0v_A at $\Omega_{i0}t = 3.0$. Here, the magnetic field lines are plotted for reference.

electrons in this region are reflected and then accelerated by the motional electric field that resulted from the fast motion of the magnetic field lines. A similar acceleration process has been thoroughly studied by Lu *et al.*[39] The speed of the corresponding electron jet in the radially outer outflow region is estimated to be about 6.0 V_A, while the speed is about 4.5 V_A in the radially inner outflow region. The speed of the electron jet in the radially outer outflow region is larger than that in the radially inner outflow region, and the situations of B_θ and E_θ are similar, where their values are larger in the radially outer part than those in the radially inner part. This is caused by the convergence of the plasma flow around $r = 0$, which leads to the asymmetry of J_{er} and B_θ between the two outflow regions.

Figure 6 plots the time evolution of the electron energy spectrum from $\Omega_{i0}t = 0$ to 3.05. Here, magnetic reconnection occurs at about $\Omega_{i0}t = 2.7$. Obviously, with the progression of magnetic reconnection, the population of energetic electrons increases rapidly. Finally, these energetic electrons form a power-law distribution with an index of about 3 at $\Omega_{i0}t = 3.05$ and the most energetic electrons can be accelerated to more than 60 times the initial thermal energy.

We also investigate the effects of the rising time of the current in the coils on magnetic reconnection between the two bubbles by keeping the peak current in the coils as $I_0 = 30\,\mathrm{kA}$. Figure 7 shows the time evolution of (a) the reconnected magnetic flux $\Phi_B/B_0 d_i$, (b) the half width of the electron current sheet δ/d_i, (c) the maximum of the electron current density $|J_{e\theta}|/en_0v_A$, and (d) the reconnection rate $\partial\Phi_B/\partial t$ when the rising times of the current in the coils are $\Omega_{i0}T_r = 1.0$, 2.0, 3.0, 4.0 and 5.0, respectively. The five vertical dotted lines represent the start time of magnetic reconnection T_m. Here, the full width at half maximum of the current sheet formed when the two magnetic bubbles approaching each other is regarded as the half width of the current sheet. Magnetic reconnection can only occur after the half width of the formed current sheet because the squeezing between the two magnetic bubbles is sufficiently small (around 0.1 d_i). For the cases with the rising time of the current in the coils $\Omega_{i0}T_r = 1.0$ and 2.0, where magnetic reconnection occurs after the current in the coils reaches its peak, the width of the

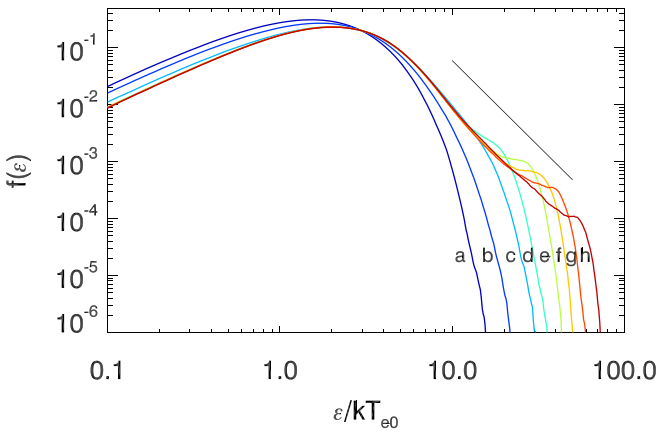

FIG. 6. The electron energy spectrum at $\Omega_i t =$ (a) 0, (b) 1.2, (c) 2.0, (d) 2.8, (e) 2.9, (f) 2.95, (g) 3.0, and (h) 3.05. The full black line represents a power-law with an index of 3.

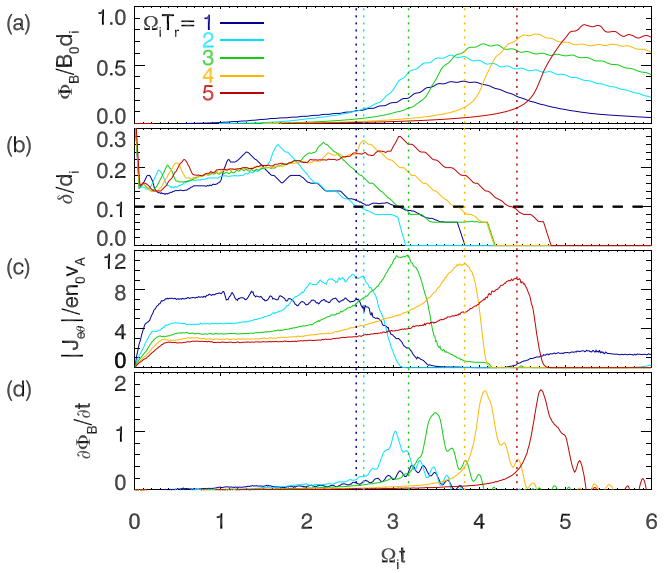

FIG. 7. The time evolution of (a) the reconnected magnetic flux $\Phi_B/B_0 d_i$, (b) the half width of the electron current sheet δ/d_i, (c) the maximum of the electron current density $|J_{e\theta}|/en_0 v_A$, and (d) the reconnection rate $\partial\Phi_B/\partial t$ when the rising times of the current in the coils are $\Omega_{i0}T_r = 1.0$, 2.0, 3.0, 4.0 and 5.0, respectively. The five vertical dotted lines represent the start time of magnetic reconnection in each case.

current sheet at first decreases linearly, and then the decrease slows down until magnetic reconnection occurs. For the cases with the rising time $\Omega_{i0}T_r = 3.0$, 4.0, and 5.0, where magnetic reconnection occurs before the current in the coils reaches its peak, the width of the current sheet decreases linearly until magnetic reconnection occurs. In general, with the increase in the rising time, magnetic reconnection occurs later. However, if normalized by the rising time, the occurrence time of magnetic reconnection becomes earlier with the increase in the rising time (shown as Table II), and the reconnected flux and the reconnection rate also become larger. The reason is that the shorter rising time will result in a faster expansion of the magnetic bubbles. During the expansion, particles are reflected and accelerated by the magnetic bubbles; they can also get Fermi acceleration when trapped between the two approaching bubbles,[40] and the acceleration will be more significant when the expanding speed becomes larger.[27] This process will lead to a stronger dissipation of the magnetic energy and smoothens the magnetic gradient in the reconnection upstream. The reconnection rate normalized by the upstream Alfven speed is about 0.1–0.8 in these cases, in agreement with previous studies.[38,41]

IV. CONCLUSIONS AND DISCUSSION

A new experimental scheme for magnetically driven reconnection is proposed in this paper and 2-D PIC simulations in the cylindrical coordinate are performed to study such kind of magnetic reconnection. Two magnetic bubbles are created by the currents in the two parallel coils and expand with the increase in the currents. When the two bubbles approach and squeeze each other, a thin current sheet is formed between them. Magnetic reconnection occurs when the current sheet is sufficiently thin. The reconnection electric field and the quadrupole Hall magnetic field in the vicinity of the X line, as well as high-speed electron jets in the outflow regions and energetic electrons with a power-law spectrum, are observed during magnetic reconnection. Also, we find that the high-speed jets and the Hall magnetic field are stronger in the radially outer outflow region than those in the radially inner outflow region because now the radially inner flow is blocked due to the plasma convergence around $r = 0$. A similar asymmetry has been reported in Inomoto *et al.*[42] In their experiment, the symmetry breaking resulted from the Hall effect associated with the toroidal field, which is different from that in our simulations.

In summary, the experimental scheme proposed in this paper may provide a new platform to study magnetic reconnection and some new characteristics are revealed with a 2-D PIC simulation model. We hope that the scheme can be experimentally realized in the future and reveal more physical characteristics about magnetic reconnection.

TABLE II. Time when magnetic reconnection occurs.

$\Omega_i T_r$	1	2	3	4	5
$\Omega_i T_m$	2.57	2.66	3.18	3.82	4.43
T_m/T_r	2.57	1.33	1.06	0.955	0.886

ACKNOWLEDGMENTS

This work was supported by 973 Program (2013CBA01503), the National Science Foundation of China (Grant Nos. 41331067, 41527804, and 11220101002), and the Key Research Program of Frontier Sciences, CAS (QYZDJ-SSW-DQC010).

[1]E. N. Parker, J. Geophys. Res. **62**, 509, https://doi.org/10.1029/JZ062i004p00509 (1957).
[2]V. M. Vasyliunas, Rev. Geophys. Space Phys. **13**, 303, https://doi.org/10.1029/RG013i001p00303 (1975).
[3]D. Biskamp, in *Magnetic Reconnection in Plasmas*, edited by M. G. Haines and K. I. Hopcraft (Cambridge University Press, Cambridge, 2000).
[4]J. Birn, J. F. Drake, M. A. Shay, B. N. Rogers, R. E. Denton, M. Hesse, M. Kuznetsova, Z. Ma, A. Bhattacharjee, A. Otto, and P. L. Pritchett, J. Geophys. Res. **106**, 3715, https://doi.org/10.1029/1999JA900449 (2001).
[5]W. Daughton, J. Scudder, and H. Karimabadi, Phys. Plasmas **13**, 072101 (2006).
[6]S. Lu, Q. Lu, C. Huang, and S. Wang, Phys. Plasmas **20**, 061203 (2013).
[7]S. Tsuneta, Astrophys. J. **456**, 840 (1996).
[8]D. N. Baker, T. I. Pulkkinen, V. Angelopoulos, W. Baumjohann, and R. L. McPherron, J. Geophys. Res. **101**, 12975, https://doi.org/10.1029/95JA03753 (1996).
[9]T. Nagai, M. Fujimoto, Y. Saito, S. Machida, T. Terasawa, R. Nakamura, T. Yamamoto, T. Mukai, A. Nishida, and S. Kokubun, J. Geophys. Res. **103**, 4419, https://doi.org/10.1029/97JA02190 (1998).
[10]V. Angelopoulos, J. P. McFadden, D. Larson, C. W. Carlson, S. B. Mende, H. Frey, T. Phan, D. G. Sibeck, K. H. Glassmeier, U. Auster, E. Donovan, I. R. Mann, I. J. Rae, C. T. Russell, A. Runov, X. Z. Zhou, and L. Kepko, Science **321**, 931 (2008).
[11]P. A. Sweet, in *IAU Symposium 6, Electro-Magnetic Phenomena in Cosmical Physics*, edited by B. Lehnert (Cambridge University Press, Cambridge, 1958), p. 123.
[12]M. Yamada, H. Ji, S. Hsu, T. Carter, R. Kulsrud, Y. Ono, and F. Perkins, Phys. Rev. Lett. **78**, 3117 (1997).
[13]Y. Ren, M. Yamada, S. Gerhardt, H. T. Ji, R. Kulsrud, and A. Kuritsyn, Phys. Rev. Lett. **95**(5), 055003 (2005).

[14]H. T. Ji, S. Terry, M. Yamada, R. Kulsrud, A. Kuritsyn, and Y. Ren, Phys. Rev. Lett. **92**, 115001 (2004).
[15]P. M. Nilson, L. Willingale, M. C. Kaluza, C. Kamperidis, S. Minardi, M. S. Wei, P. Fernandes, M. Notley, S. Bandyopadhyay, M. Sherlock, R. J. Kingham, M. Tatarakis, Z. Najmudin, W. Rozmus, R. G. Evans, M. G. Haines, A. E. Dangor, and K. Krushelnick, Phys. Rev. Lett. **97**, 255001 (2006).
[16]C. K. Li, F. H. Seguin, J. A. Frenje, J. R. Rygg, R. D. Petrasso, R. P. J. Town, P. A. Amendt, S. P. Hatchett, O. L. Landen, A. J. Mackinnon, P. K. Patel, M. Tabak, J. P. Knauer, T. C. Sangster, and V. A. Smalyuk, Phys. Rev. Lett. **99**, 015001 (2007).
[17]J. Y. Zhong, Y. T. Li, X. G. Wang, J. Q. Wang, Q. L. Dong, C. J. Xiao, S. J. Wang, X. Liu, L. Zhang, L. An, F. L. Wang, J. Q. Zhu, Y. Gu, X. T. He, G. Zhao, and J. Zhang, Nat. Phys. **6**, 984 (2010).
[18]Q. L. Dong, S. J. Wang, Q. M. Lu, C. Huang, D. W. Yuan, X. Liu, X. X. Lin, Y. Li, H. G. Wei, J. Y. Zhong, J. R. Shi, S. E. Jiang, Y. K. Ding, B. B. Jiang, K. Du, X. T. He, M. Y. Yu, C. S. Liu, S. Wang, Y. J. Tang, J. Q. Zhu, G. Zhao, Z. M. Sheng, and J. Zhang, Phys. Rev. Lett. **108**, 215001 (2012).
[19]W. Fox, A. Bhattacharjee, and K. Germaschewski, Phys. Plasmas **19**, 056309 (2012).
[20]S. Lu, Q. M. Lu, Q. L. Dong, C. Huang, S. Wang, J. Q. Zhu, Z. M. Sheng, and J. Zhang, Phys. Plasmas **20**, 112110 (2013).
[21]S. R. Totorica, T. Abel, and F. Fiuza, Phys. Rev. Lett. **116**, 095003 (2016).
[22]Z. Xu, B. Qiao, H. X. Chang, W. P. Yao, S. Z. Wu, X. Q. Yan, C. T. Zhou, X. G. Wang, and X. T. He, Phys. Rev. E **93**, 033206 (2016).
[23]W. Fox, J. Park, W. Deng, G. Fiksel, A. Spitkovsky, and A. Bhattacharjee, Phys. Plasmas **24**(9), 092901 (2017).
[24]S. R. Totorica, T. Abel, and F. Fiuza, Phys. Plasmas **24**(4), 041408 (2017).
[25]X. R. Fu, Q. M. Lu, and S. Wang, Phys. Plasmas **13**, 012309 (2006).
[26]J. F. Drake, M. Swisdak, H. Che, and M. A. Shay, Nature **443**, 553 (2006).
[27]K. Huang, Q. M. Lu, C. Huang, Q. L. Dong, H. Y. Wang, F. B. Fan, Z. M. Sheng, S. Wang, and J. Zhang, Phys. Plasmas **24**, 102101 (2017).
[28]F. Guo, H. Li, W. Daughton, and Y. H. Liu, Phys. Rev. Lett. **113**, 155005 (2014).
[29]X. Li, F. Guo, H. Li, and G. Li, Astrophys. J. Lett. **811**(2), L24 (2015).
[30]G. Fiksel, W. Fox, A. Bhattacharjee, D. H. Barnak, P. Y. Chang, K. Germaschewski, S. X. Hu, and P. M. Nilson, Phys. Rev. Lett. **113**(10), 105003 (2014).
[31]X. X. Pei, J. Y. Zhong, Y. Sakawa, Z. Zhang, K. Zhang, H. G. Wei, Y. T. Li, Y. F. Li, B. J. Zhu, T. Sano, Y. Hara, S. Kondo, S. Fujioka, G. Y. Liang, F. L. Wang, and G. Zhao, Phys. Plasmas **23**(3), 032125 (2016).
[32]H. Daido, F. Miki, K. Mima, M. Fujita, K. Sawai, H. Fujita, Y. Kitagawa, S. Nakai, and C. Yamanaka, Phys. Rev. Lett. **56**(8), 846 (1986).
[33]C. Courtois, A. D. Ash, D. M. Chambers, R. A. D. Grundy, and N. C. Woolsey, J. Appl. Phys. **98**(5), 054913 (2005).
[34]S. Fujioka, Z. Zhang, K. Ishihara, K. Shigemori, Y. Hironaka, T. Johzaki, A. Sunahara, N. Yamamoto, H. Nakashima, T. Watanabe, H. Shiraga, H. Nishimura, and H. Azechi, Sci. Rep. **3**, 1170 (2013).
[35]L. Gao, H. Ji, G. Fiksel, W. Fox, M. Evans, and N. Alfonso, Phys. Plasmas **23**(4), 043106 (2016).
[36]G. Fiksel, W. Fox, L. Gao, and H. T. Ji, Appl. Phys. Lett. **109**, 134103 (2016).
[37]Z. W. Yang, Q. M. Lu, B. Lembège, and S. Wang, J. Geophys. Res. **114**, A03111, https://doi.org/10.1029/2008JA013785 (2009).
[38]K. Huang, C. Huang, Q. L. Dong, Q. M. Lu, S. Lu, Z. M. Sheng, S. Wang, and J. Zhang, Phys. Plasmas **24**, 041406 (2017).
[39]S. Lu, Q. M. Lu, C. Huang, Q. L. Dong, J. Q. Zhu, Z. M. Sheng, S. Wang, and J. Zhang, New J. Phys. **16**, 083021 (2014).
[40]S. Lu, Q. M. Lu, F. Guo, Z. M. Sheng, H. Y. Wang, and S. Wang, New. J. Phys. **18**, 013501 (2016).
[41]W. Fox, A. Bhattacharjee, and K. Germaschewski, Phys. Rev. Lett. **106**(21), 215003 (2011).
[42]M. Inomoto, S. P. Gerhardt, M. Yamada, H. Ji, E. Belova, A. Kuritsyn, and Y. Ren, Phys. Rev. Lett. **97**(13), 135002 (2006).